



INSTITUT NATIONAL DE RECHERCHE EN INFORMATIQUE ET EN AUTOMATIQUE

*New Cardiovascular Indices Based on a Nonlinear
Spectral Analysis of Arterial Blood Pressure
Waveforms*

Taous-Meriem Laleg — Claire Médigue — Yves Papelier — Emmanuelle Crépeau —
Michel Sorine

N° 6312

Octobre 2007

Thème BIO

 *rapport
de recherche*

arXiv:0710.0280v2 [math-ph] 2 Oct 2007



New Cardiovascular Indices Based on a Nonlinear Spectral Analysis of Arterial Blood Pressure Waveforms

Taous-Meriem Laleg , Claire Médigue , Yves Papelier , Emmanuelle Crépeau
, Michel Sorine

Thème BIO — Systèmes biologiques
Projet SISYPHE

Rapport de recherche n° 6312 — Octobre 2007 — 26 pages

Abstract: A new method for analyzing arterial blood pressure is presented in this report. The technique is based on the scattering transform and consists in solving the spectral problem associated to a one-dimensional Schrödinger operator with a potential depending linearly upon the pressure. This potential is then expressed with the discrete spectrum which includes negative eigenvalues and corresponds to the interacting components of an N-soliton. The approach is similar to a nonlinear Fourier transform where the solitons play the role of sine and cosine components. The method provides new cardiovascular indices that seem to contain relevant physiological information. We first show how to use this approach to decompose the arterial blood pressure pulse into elementary waves and to reconstruct it or to separate its systolic and diastolic phases. Then we analyse the parameters computed from this technique in two physiological conditions, the head-up 60 degrees tilt test and the isometric handgrip test, widely used for studying short term cardiovascular control. Promising results are obtained.

Key-words: Blood pressure, scattering transform, solitons, cardiovascular indices

Nouveaux indices cardio-vasculaires basés sur une analyse spectrale non linéaire de la forme des ondes de pression artérielle

Résumé : Une nouvelle méthode d'analyse du signal de pression artérielle est proposée dans ce rapport. La technique est basée sur la transformation scattering et consiste à résoudre un problème spectral associé à l'opérateur de Schrodinger unidimensionnel avec un potentiel qui dépend linéairement de la pression. Le potentiel est reconstruit à l'aide du spectre discret uniquement qui comprend des valeurs propres négatives correspondant à N solitons en interaction. L'approche est analogue à une transformée de Fourier où les solitons jouent le rôle des composantes sinus et cosinus. La méthode introduit de nouveaux indices cardio-vasculaires qui semblent contenir des informations physiologiques intéressantes. Dans un premier temps, nous appliquons la méthode à la décomposition du signal de pression artérielle en ondes élémentaires et à sa reconstruction ou à la séparation de ses parties diastolique et systolique. Nous analysons par la suite les paramètres calculés à partir de cette technique dans deux conditions physiologiques généralement utilisées pour l'étude du contrôle cardio-vasculaire à court-terme: test d'inclinaison à 60 degrés et exercice isométrique (handgrip). Des résultats prometteurs ont été obtenus.

Mots-clés : Pression artérielle, transformation scattering, solitons, indices cardio-vasculaires

Contents

| | | |
|----------|-----------------------------------------------------------|-----------|
| 1 | Introduction | 4 |
| 2 | A scattering-based signal analysis method | 5 |
| 2.1 | Scattering transform for a Schrödinger equation | 5 |
| 2.2 | A scattering based signal analysis method | 7 |
| 2.3 | SBSA and the invariants of KdV | 8 |
| 3 | Application of the SBSA to the ABP waves | 11 |
| 3.1 | ABP reconstruction | 11 |
| 3.2 | Separation of the systolic and diastolic phases | 11 |
| 4 | New spectral cardiovascular indices | 13 |
| 4.1 | The SBSA parameters and the ABP | 13 |
| 4.2 | Head-up 60 degrees tilt-test | 15 |
| 4.3 | Isometric handgrip exercise | 16 |
| 5 | Conclusion | 22 |

1 Introduction

The analysis of mean values and beat-to-beat variability of cardiovascular (CV) time series has been widely used as a noninvasive approach to study the control of the autonomic nervous system (ANS) on the CV function [2], [28]. CV time series usually give information in the frequency and amplitude domains. The frequency (or period) is given by the RR interval (between two R peaks on the ECG) or the pulse interval (PI) (between two systolic blood pressure peaks). The amplitude concerns systolic, diastolic and mean pressures (noted SBP, DBP and MBP respectively). Standard measures of these parameters are mean levels and global variability, spectral, temporal and time-frequency analysis [33].

Instead of the usual decomposition of the arterial blood pressure (ABP) waveform into a linear superposition of harmonic waves (sine and cosine functions) [40], [46], in this article we propose to use nonlinear superpositions of particular travelling waves, the N-solitons-solutions of the Korteweg-de Vries (KdV) equation where N travelling components are interacting. These N-solitons play the role here of the harmonic-waves solutions of the linear wave equation. The concept of soliton refers in fact to a solitary wave emerging unchanged in shape and speed from the collision with other solitary waves [38]. They fascinate scientists by their very interesting coherent-structure characteristics and are used in many fields to model natural phenomena. Solitons are solutions of nonlinear dispersive equations like the KdV equation arising in a variety of physical problems, for example to describe wave motion in shallow water canals [39], [49]. The use of solitons to describe the ABP was already introduced in [48] and [35] where a KdV equation and a Boussinesq equation were respectively proposed as a blood flow model. Recently, in [9], [24] a reduced model of the ABP cycle was introduced. The latter consists of a sum of a 2 or 3-soliton solution of a KdV equation, describing fast phenomena during the systolic phase and a 2-element windkessel model describing slow phenomena during the diastolic phase. We recall that the systolic phase corresponds to the contraction of the heart, driving blood out of the left ventricle while the diastolic phase corresponds to the period of relaxation of the heart.

The decomposition of the ABP signal into a nonlinear superposition of solitons introduced in this article is based on an elegant mathematical transform: the scattering transform for a one-dimensional Schrödinger equation [6], [12], [14]. The main idea in our utilization of this transform consists in interpreting the pressure as a potential able to attract or repulse "fluid particles" or equivalently to transmit or reflect waves associated with them. This situation is modelled by a one-dimensional Schrödinger operator with a potential depending linearly upon the pressure wave [25]. The discrete levels of energy or speed of this system are given by the discrete spectrum of the Schrödinger operator. The associated eigenstates describe some coherent structures that are present in the pressure waveform and expressed as N solitons.

The scattering-based signal analysis (SBSA) method introduces a new spectral description of the pressure waveform leading to new cardiovascular indices. This study aims to

analyse these new parameters in two physiological conditions that are widely used for studying the short term control of the CV system: the head-up 60 degrees tilt test, in 15 healthy subjects, and the isometric handgrip exercise, in 13 healthy subjects.

Among the SBSA parameters, some invariants of the scattering transform seem to be related to the contraction strength of the left ventricle and the stroke volume (SV). Moreover, the beat-to-beat relation between the first eigenvalue and the heart period might be more reliable than the baroreflex slope for distinguishing two conditions.

In the next section, we present the basis of the SBSA method. Section III compares real and reconstructed pressures using the SBSA and shows how we can separate the fast and slow pressure components related to the systolic and diastolic phases respectively. Section IV introduces the new cardiovascular indices computed using the SBSA technique and presents the results of the analysis in two physiological conditions: tilt and handgrip, including a discussion. Finally a conclusion summarizes the different results.

2 A scattering-based signal analysis method

In this section, we introduce a new signal analysis method based on the scattering theory. We start by briefly recalling the basis of the Direct and Inverse Scattering Transforms (DST & IST). Then, we present the main idea in the SBSA technique. For more details about DST and IST the reader can refer to the abundant literature and the references given.

2.1 Scattering transform for a Schrödinger equation

Let V be a given real function in the so-called Faddeev class $L_1^1(\mathbb{R})$ [1]:

$$L_1^1(\mathbb{R}) = \{V \in L^1(\mathbb{R}), \int_{-\infty}^{+\infty} |V(x)|(1 + |x|)dx < \infty\}. \quad (1)$$

We consider the one dimensional Schrödinger operator $H(V)$ with a potential V :

$$H(V) : \psi \rightarrow H(V)\psi = -\frac{\partial^2 \psi}{\partial x^2} + V\psi. \quad (2)$$

The DST of V will be defined as a function of the solution of the spectral problem for $H(V)$ where λ and ψ are respectively the eigenvalues and the associate eigenfunctions for some normalization:

$$H(V)\psi = \lambda\psi. \quad (3)$$

The spectrum of $H(V)$ has two components: a continuous spectrum equal to $(0, +\infty)$ and a discrete spectrum with negative eigenvalues [11], [12], [14].

For the positive eigenvalues denoted here $\lambda = k^2$, there are eigenfunctions, called scattering solutions of (3) consisting of linear combinations of $\exp(ikx)$ and $\exp(-ikx)$ as $x \rightarrow \pm\infty$. Among them, we consider the Jost solutions from the left f_l and from the right f_r , normalized at $\pm\infty$:

$$H(V)f_j = k^2 f_j, \quad k \in \mathbb{R} \setminus \{0\}, \quad j = l, r, \quad (4)$$

$$\exp(-ikx)f_l(k, x) = 1 + o(1), \quad x \rightarrow +\infty, \quad (5)$$

$$\exp(-ikx)\frac{\partial f_l(k, x)}{\partial x} = ik + o(1), \quad x \rightarrow +\infty, \quad (6)$$

$$\exp(+ikx)f_r(k, x) = 1 + o(1), \quad x \rightarrow -\infty, \quad (7)$$

$$\exp(+ikx)\frac{\partial f_r(k, x)}{\partial x} = -ik + o(1), \quad x \rightarrow -\infty, \quad (8)$$

We recall that, for each fixed $x \in \mathbb{R}$ the Jost solutions have analytic extensions in k to the upper-half complex plane [1].

The transmission coefficient T and the reflection coefficients R_l and R_r from the left and from the right respectively are defined through the relations:

$$f_l(k, x) = \frac{\exp(ikx)}{T(k)} + \frac{R_l(k)\exp(-ikx)}{T(k)} + o(1), \quad x \rightarrow -\infty, \quad (9)$$

$$f_r(k, x) = \frac{\exp(-ikx)}{T(k)} + \frac{R_r(k)\exp(ikx)}{T(k)} + o(1), \quad x \rightarrow +\infty, \quad (10)$$

These coefficients satisfy:

$$|T(k)|^2 + |R_l(k)|^2 = |T(k)|^2 + |R_r(k)|^2 = 1. \quad (11)$$

On the other hand, for the negative eigenvalues of the discrete spectrum, equation (3) admits solutions called bound states that belong to $L^2(\mathbb{R})$ in the x variable. When V belongs to the Faddeev class, the bound states solutions of (3) decay exponentially as $x \rightarrow \pm\infty$ and their number N is finite [1]. Let us denote $\lambda_n = -\kappa_n^2$ with $\lambda_1 \leq \lambda_2 \leq \dots$ and ψ_n the N negative eigenvalues and L^2 -normalized bound states:

$$H(V)\psi_n = -\kappa_n^2\psi_n, \quad \int_{-\infty}^{+\infty} |\psi_n(x)|^2 dx = 1, \quad n = 1, \dots, N. \quad (12)$$

The eigenspaces being of dimension 1, the bound states and the Jost solutions are proportional:

$$\psi_n(x) = c_{ln}f_l(i\kappa_n, x) = (-1)^{N-n}c_{rn}f_r(i\kappa_n, x), \quad (13)$$

where c_{ln} and c_{rn} are called the bound-state norming constants and are defined by:

$$c_{jn} := \left[\int_{-\infty}^{+\infty} |f_j(i\kappa_n, x)|^2 dx \right]^{-\frac{1}{2}}, \quad j = l, r. \quad (14)$$

We now define the DST of V as the sets of scattering data from the left, $\mathcal{S}_l(V)$ or from the right, $\mathcal{S}_r(V)$:

$$\mathcal{S}_j(V) := \{R_j, \kappa_n, c_{\bar{j}n}, n = 1, \dots, N\}, \quad \{j, \bar{j}\} = \{l, r\}. \quad (15)$$

The potential can be uniquely reconstructed by using any one of these sets. The solution of this inverse problem, called IST, is the object of many studies concerned with specific classes of potentials [1], [7], [11], [15], [29]. Two transforms are then available, \mathcal{S} and \mathcal{S}^{-1} (in the sequel we choose $j = r$ and drop the subscripts r and l for simplicity).

In this study, we will use the special class of *reflectionless potentials* for which the left or right reflection coefficients are zero. Such potentials can be constructed as follows: let Π_d be the projector zeroing the R -component of $\mathcal{S}(V)$, then $\mathcal{S}^{-1} \circ \Pi_d \circ \mathcal{S}(V)$ is reflectionless for any V in the Faddeev class. There are useful explicit representations of reflectionless potentials using only the discrete spectrum as in the following theorem [14]:

Theorem: If V is reflectionless for $H(V)$, then:

$$V(x) = -4 \sum_{n=1}^N \kappa_n \psi_n^2(x), \quad x \in \mathbb{R}. \quad (16)$$

V can be also written:

$$V(x) = -2 \frac{\partial^2 (\log (\det(I + A)))}{\partial x^2}, \quad x \in \mathbb{R}, \quad (17)$$

where A is an $N \times N$ matrix:

$$A(x) = \left[\frac{c_m c_n}{\kappa_m + \kappa_n} \exp((\kappa_m + \kappa_n)x) \right], \quad n, m = 1, \dots, N. \quad (18)$$

Note that in (17) and (18), the potential is entirely defined with $2N$ parameters namely κ_n and c_n , $n = 1, \dots, N$.

A very close relation between a soliton solution of a KdV equation and a reflectionless potential of the Schrödinger operator was introduced in [14]. In fact these potentials remain reflectionless when evolving in time and space according to a KdV equation. For $t \rightarrow +\infty$, N 1-solitons emerge, each one being characterized by a pair (κ_n, c_n) such that $4\kappa_n^2$ gives the speed of the soliton and c_n its position. Therefore each component $-4\kappa_n \psi_n^2$ in the sum (16) refers to a single soliton.

2.2 A scattering based signal analysis method

We now present how to use IST in a seemingly new method to analyse pulse-like signals of the Faddeev class.

The main idea in the SBSA approach is to interpret a positive signal y in the Faddeev class as a quantum well by changing the sign, and to tune the depth of this well with a positive parameter χ in order to approximate y by a coherent state y_χ . For a deeper well the trapped energy will be higher and the approximation better, as we will prove. The estimate is then obtained by filtering out the nonlinear reflections:

$$y_\chi = -\frac{1}{\chi} \mathcal{S}^{-1} \circ \Pi_d \circ \mathcal{S}(-\chi y). \quad (19)$$

A convenient explicit formula is available, χy_χ being a reflectionless potential:

$$y_\chi = \frac{4}{\chi} \sum_{n=1}^{N_\chi} \kappa_{\chi,n} \psi_{\chi,n}^2, \quad (20)$$

where $-\kappa_{\chi,n}^2$ and $\psi_{\chi,n}$, $n = 1, \dots, N_\chi$ are the negative eigenvalues and the associated L^2 -normalized eigenfunctions for $H(-\chi y)$.

Then, we look for a value $\hat{\chi}$ for the parameter χ such that the signal y is well approximated by $y_{\hat{\chi}}$. This is the decomposition of the signal y into the nonlinear superposition of solitons announced in [25].

It is well-known that the number of negative eigenvalues N_χ of $H(-\chi y)$ is a nondecreasing function of χ and there is an infinite unbounded sequence (χ_n) such that $N_{\chi_n} = N_{\chi_{n-1}} + 1$ [25], [31]. Determining the parameter $\hat{\chi}$ determines the number of negative eigenvalues and hence the number of solitons components required for a satisfying approximation of the signal y . Fig. 1 summarizes the SBSA technique.

2.3 SBSA and the invariants of KdV

The scattering transform has an infinite number of invariants which are related to the KdV conserved quantities [14], [32]. Let us denote these invariants $I_m(V)$, $m = 0, 1, 2, \dots$. They are of the form (we take $-V$ as argument having (19) in mind):

$$I_m(-V) = (-1)^{m+1} \frac{2m+1}{2^{2m+2}} \int_{-\infty}^{+\infty} P_m(V, \frac{\partial V}{\partial x}, \frac{\partial^2 V}{\partial x^2}, \dots) dx, \quad (21)$$

where P_m , $m = 0, 1, 2, \dots$ are known polynomials in V and its successive derivatives with respect to $x \in \mathbb{R}$ [6].

A general formula relating $I_m(-V_\chi)$, with $V_\chi = -\chi y$, to the scattering data of $H(V_\chi)$ can be deduced; see for example [6], [16], [32]:

$$I_m(\chi y) = \sum_{n=1}^{N_\chi} \kappa_{\chi,n}^{2m+1} + \frac{2m+1}{2\pi} \int_{-\infty}^{+\infty} (-k^2)^m \ln(|T_\chi(k)|) dk, \quad (22)$$

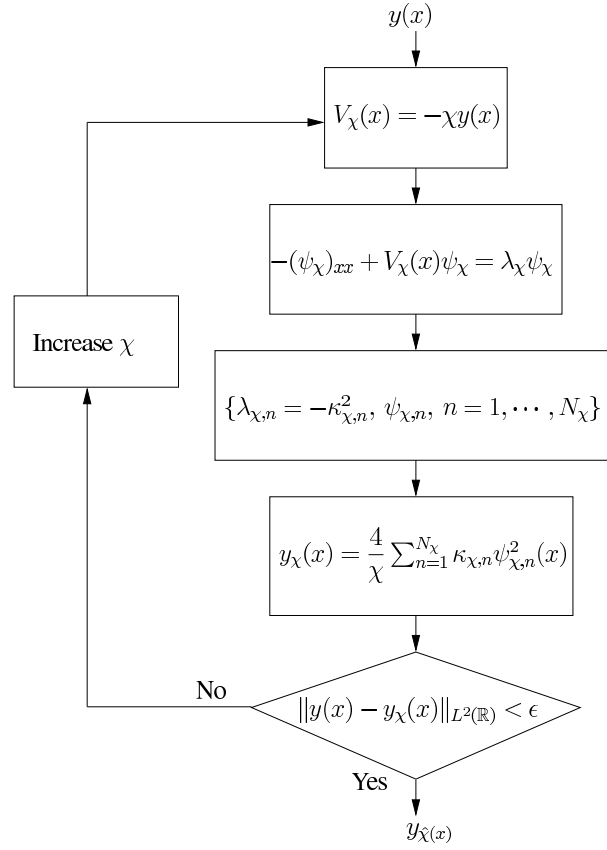


Figure 1: Signals analysis with the SBSA method

$m = 0, 1, 2, \dots$.

We introduce the Riesz means of the negative eigenvalues λ_n of $H(V)$ such that $\lambda_n \leq \lambda \leq 0$:

$$S_{\gamma, \lambda}(-V) = \sum_{\lambda_n \leq \lambda} |\lambda_n|^\gamma, \quad \gamma \geq 0. \quad (23)$$

Remark that $S_{0, \lambda}(V)$ is the number of eigenvalues of $H(V)$ smaller than λ .

For an N_χ -soliton, for instance $-\chi y_\chi$ of the previous subsection, the invariants only depend on the discrete spectrum and they are related to the Riesz means as follows:

$$I_m(\chi y_\chi) = S_{\gamma,0}(\chi y_\chi), \quad \gamma = m + \frac{1}{2}, \quad m = 0, 1, 2, \dots \quad (24)$$

A "sum rule" is then verified by the invariants of χy and χy_χ :

$$I_m(\chi y) = I_m(\chi y_\chi) + \frac{2m+1}{2\pi} \int_{-\infty}^{+\infty} (-k^2)^m \ln(|T_\chi(k)|) dk, \quad (25)$$

$m = 0, 1, 2, \dots$.

In this article we are only interested in the two first invariants ($m = 0$ and $m = 1$) corresponding to the conservation of mass and momentum for the KdV flows. Here it is sufficient to see them as invariants of the DST, in the same manner energy is invariant for the Fourier transform (Plancherel's theorem). We will show later in the application of the SBSA to the ABP that these two invariants are related to some important cardiovascular parameters.

So, for $m = 0$, $P_0(V_\chi, \dots) = V_\chi$, we get with (21) and (25):

$$\int_{-\infty}^{+\infty} y dx = \int_{-\infty}^{+\infty} y_\chi dx + \frac{2}{\pi\chi} \int_{-\infty}^{+\infty} \ln(|T_\chi(k)|) dk. \quad (26)$$

For $m = 1$, $P_1(V_\chi, \dots) = V_\chi^2$, we have with (21) and (25):

$$\int_{-\infty}^{+\infty} y^2 dx = \int_{-\infty}^{+\infty} y_\chi^2 dx - \frac{8}{\pi\chi^2} \int_{-\infty}^{+\infty} k^2 \ln(|T_\chi(k)|) dk. \quad (27)$$

Equation (27) is known as the Buslaev-Faddeev-Zakharov trace formula.

Proposition: Let $y : \mathbb{R} \rightarrow \mathbb{R}$ be a continuous non-negative function with a compact support, then we have the convergence of the estimates of the first two invariants:

$$\lim_{\chi \rightarrow +\infty} I_m(y_\chi) = I_m(y), \quad m = 0, 1. \quad (28)$$

Proof: We can apply the results on the Lieb-Thirring semiclassical limit of the Riesz means [4], [20], [21], [26]:

$$\lim_{\chi \rightarrow +\infty} \frac{S_{\gamma,0}(\chi y)}{\chi^{\frac{1}{2}+\gamma}} = L_\gamma^{cl} \int_{\mathbb{R}} y(x)^{\frac{1}{2}+\gamma} dx, \quad \gamma \geq \frac{1}{2}, \quad (29)$$

where L_γ^{cl} is the so-called Lieb-Thirring constant given by:

$$L_\gamma^{cl} \equiv (4\pi)^{-\frac{1}{2}} \frac{\Gamma(\gamma+1)}{\Gamma(\gamma+\frac{3}{2})}. \quad (30)$$

We notice that for $\gamma = \frac{1}{2}$:

$$\lim_{\chi \rightarrow +\infty} \frac{S_{\frac{1}{2},0}(\chi y)}{\chi} = L_{\frac{1}{2}}^{cl} \int_{\mathbb{R}} y(x) dx, \quad L_{\frac{1}{2}}^{cl} = \frac{1}{4}. \quad (31)$$

So, we deduce the convergence of the first invariant estimate.

For $\gamma = \frac{3}{2}$ we have an analog of the Plancherel identity for the Fourier transform:

$$\lim_{\chi \rightarrow +\infty} \frac{S_{\frac{3}{2},0}(\chi y)}{\chi^2} = L_{\frac{3}{2}}^{cl} \int_{\mathbb{R}} y(x)^2 dx, \quad L_{\frac{3}{2}}^{cl} = \frac{3}{16}. \quad (32)$$

Therefore, we get the convergence of the second invariant.

3 Application of the SBSA to the ABP waves

3.1 ABP reconstruction

In the previous subsection, we presented a new signal analysis method based on the scattering transform. Now, we propose to use this method for ABP analysis. For convenience we replace the space variable x by the time variable t .

We note the ABP signal $P(t)$ and the estimated pressure with the SBSA technique $\hat{P}(t)$ such that:

$$\hat{P}(t) = \frac{4}{\chi} \sum_{n=1}^{N_\chi} \kappa_{\chi,n} \psi_{\chi,n}^2(t), \quad (33)$$

where $-\kappa_{\chi,n}^2$ and $\psi_{\chi,n}$, $n = 1, \dots, N_\chi$ are the N_χ negative eigenvalues and associated L^2 -normalized eigenfunctions of $H(-\chi P)$. We recall that each component $4\kappa_{\chi,n} \psi_{\chi,n}^2$ in (33) refers to a single soliton [14], [25].

In Fig. 2 and Fig. 3, measured and reconstructed pressures at the aorta and at the finger levels are presented respectively. The aortic pressure was measured using a catheter while a Finapres was used to measure the pressure at finger. Only 5 to 10 components are sufficient for a good reconstruction of the ABP waveform.

3.2 Separation of the systolic and diastolic phases

Following the work done in [9], [24], we propose here using the SBSA technique to separate the pressure into fast and slow parts corresponding respectively to the systolic and diastolic phases. Indeed a reduced model of ABP has been proposed in [9], [24]. The latter consists of

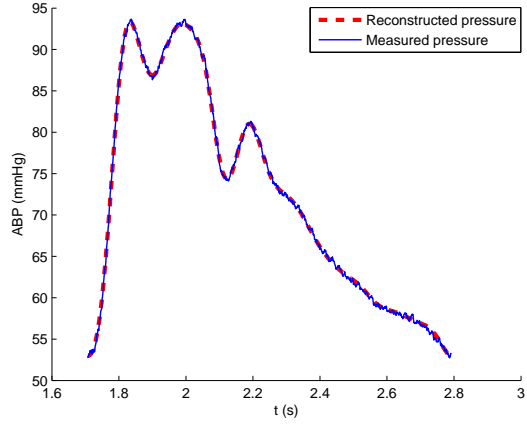


Figure 2: Measured and reconstructed pressure at the aorta

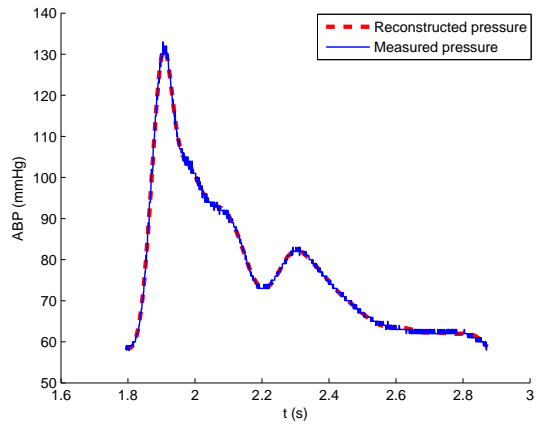


Figure 3: Measured and reconstructed pressure at the finger

a sum of two terms: a 2 or 3-soliton solution of a KdV equation describing fast phenomena which predominate during the systolic phase and a 2-element windkessel model describing slow phenomena during the diastolic phase. As noticed in the previous section, the SBSA technique decomposes the ABP signal into a sum of solitons, each one characterized by its velocity given by the discrete eigenvalues $-\kappa_{\chi,n}^2$. So the largest $\kappa_{\chi,n}^2$, $n = 1, \dots, N_s$ describe

fast phenomena while the smallest ones describe slow phenomena. Referring to [9], [24], we take $N_s = 2$ or 3 . We note \hat{P}_s and \hat{P}_d the estimated systolic and diastolic pressures respectively such that:

$$\hat{P}_s(t) = \frac{4}{\chi} \sum_{n=1}^{N_s} \kappa_{\chi,n} \psi_{\chi,n}^2, \quad \hat{P}_d(t) = \frac{4}{\chi} \sum_{n=N_s+1}^{N_x} \kappa_{\chi,n} \psi_{\chi,n}^2. \quad (34)$$

We compute the first two invariants of these partial pressures with the Riesz means for the chosen cut-off speed λ :

$$INV_1(\lambda) = \frac{4}{\chi} S_{\frac{1}{2},\lambda}(\chi P), \quad INV_2(\lambda) = \frac{16}{3\chi^2} S_{\frac{3}{2},\lambda}(\chi P), \quad (35)$$

We can now define the proposed invariants for the whole beat and for the systolic and diastolic phases (INV_j , $INVS_j$, $INVD_j$, $j = 1, 2$ respectively):

$$\begin{cases} INV_j = INV_j(0), \\ INVS_j = INV_j(\lambda_s), \\ INVD_j = INV_j(0) - INVS_j(\lambda_s), \end{cases} \quad j = 1, 2, \quad (36)$$

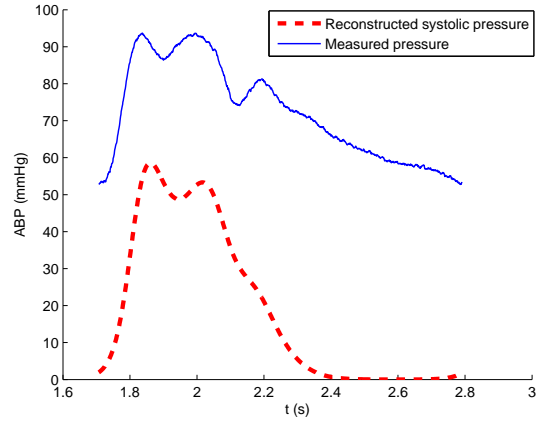
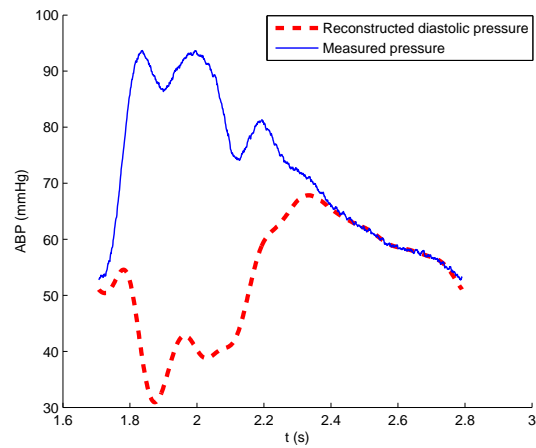
where $\lambda_s = \lambda_{\chi,2}$ or $\lambda_{\chi,3}$.

In Fig. 4 and Fig. 5, we represent the measured pressure and the estimated systolic and diastolic parts respectively. We remark that \hat{P}_s and \hat{P}_d are respectively localized during the systole and the diastole, as expected.

4 New spectral cardiovascular indices

4.1 The SBSA parameters and the ABP

The SBSA technique provides a new description of the ABP signal using the DST. As seen in the previous section, the reconstruction of the signal by IST from its spectral data gives good results. Instead of reconstructing the original signal, it is possible to modify the spectrum leading to some kind of filtering. This is illustrated by the separation of the systolic and diastolic phases. Moreover, the SBSA method introduces new parameters. The first two global invariants INV_1 and INV_2 are respectively, by definition, the usual mean blood pressure (MBP) and the less usual, but easy to compute directly, integral of the square of the pressure. The first systolic invariant $INVS_1$ is a new index: we think that it can be correlated to SV. Remark that if INV_2 is easy to compute directly, the "fast part" of this integral, the second systolic invariant $INVS_2$ is a new less obvious index and might contain information on ventricular contractility. SV and contractility are in fact parameters of great interest that are difficult to measure routinely, as they require invasive or sophisticated

Figure 4: \hat{P}_s and fast systolic phenomenaFigure 5: \hat{P}_d and slow diastolic phenomena

techniques. For instance SV can be estimated by invasive nuclear ventriculography [47], 2D echocardiography [23], radionuclide monitoring [43], impedance cardiography [8], [10]. Only one evaluation of SV from ABP has been proposed [19]. Ventricular contractility is assessed by the mean of the tissue doppler echocardiography [17], [18].

On the other hand, the eigenvalues computed with the SBSA technique are strongly dependent upon the ABP waveform. Indeed, when the pressure waveform changes, the optimal value of the parameter χ and the eigenvalues also change. This fact is illustrated in Fig. 6. Therefore, the eigenvalues could be used to assess the baroreflex sensitivity (BRS) in a certain way. In fact, the BRS expresses the variation of the heart beat interval in response to each arterial pressure variation. The BRS concept was first based on drug-induced responses of ABP and heart period [37]. Then various time [27], [34], [36] and spectral [5], [28], [34], domain methods [27] were compared.

In this section we analyse the SBSA parameters in two situations, devoted to the assessment of the ANS control of the CV system. We restrict the study to the modulus of the first two negative eigenvalues $|\lambda_{\chi,1}| = |\lambda_1|$, $|\lambda_{\chi,2}| = |\lambda_2|$ and the first two invariants (global, systolic and diastolic). We include in the analysis some classical parameters which are PI, SBP and DBP.

4.2 Head-up 60 degrees tilt-test

The head-up tilt test is mainly used for vasovagal syncope diagnosis, characterized by an autonomic dysfunction. It consists in the orthostatic transition from the supine to the standing positions. This leads to a redistribution of the venous blood volume, from the intrathoracic region towards the venous volume in the leg and lower abdominal veins. This leads to a decrease in SV and PI and an increase in SBP [10], [41], [42], [44].

A group of 15 healthy subjects under 0.25Hz paced breathing, already studied [3], was considered. The table was rotated to an upright position at 60 degrees. The continuous ABP was measured at the finger using a Finapres device [45]. The two positions, supine and standing, were compared using the Wilcoxon non parametric paired test.

Fig. 7 shows the time series of PI, SBP, $INVS_1$ and $|\lambda_1|$ in the supine and standing positions. Mean levels of the ABP parameters are presented in Table 1. We notice that significant differences between the supine and standing positions appear for PI, DBP, $|\lambda_1|$, $|\lambda_2|$ and $INVS_1$ while for the other parameters the differences are not significant. So after the tilt test, SBP and MBP recover their prior values (preceding the tilt phase) whereas $INVS_1$ is decreased. If $INVS_1$ is related to SV then this means that SV remains decreased after the tilt test and this can be explained by the decrease in the venous return.

The ABP analysis during the transition from the supine to the standing positions was possible for only nine subjects. For these, we assessed the linear relation between PI of the beat $n + 1$ and $|\lambda_1|$ computed for the beat n . In Fig. 8, we note that as PI decreases, $|\lambda_1|$ increases and that the linear correlation between PI and $|\lambda_1|$ is stronger around the transition than in supine position. Table 2 shows that the correlation coefficient (R^2) and the slope, compared by a one-way repeated measures analysis of variance, were significantly

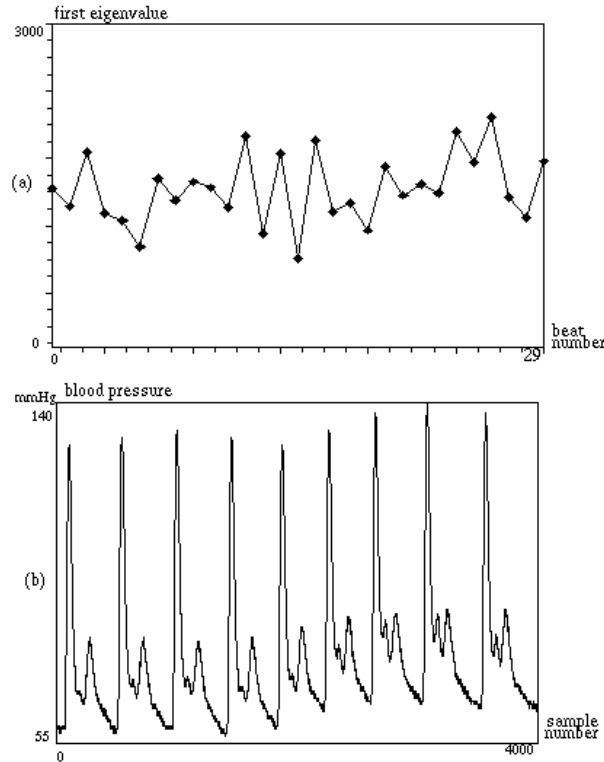


Figure 6: (a) First eigenvalue time series of a healthy subjects under $0.25Hz$ paced-breathing during 29 beats. The signal exhibits a beat-to-beat variability that is twice as fast as the breathing rate. (b) A zoom on a few beats shows morphological changes in the blood pressure signal.

stronger around the transition than in supine or standing positions. Moreover, a comparison with usual BRS indices, SBP and pulse pressure (PP), shows that $|\lambda_1|$ has the strongest correlation with PI (Table 3). It is not surprising that $|\lambda_1|$ is more informative about the relation between the heart period and the ABP because it reflects the arterial waveform and not only one (SBP) or two (PP) samples of this waveform.

4.3 Isometric handgrip exercise

The isometric handgrip exercise is mainly used for the evaluation of a non appropriate ANS behavior, that mimics actual conditions of professional or domestic exposure, with arterial

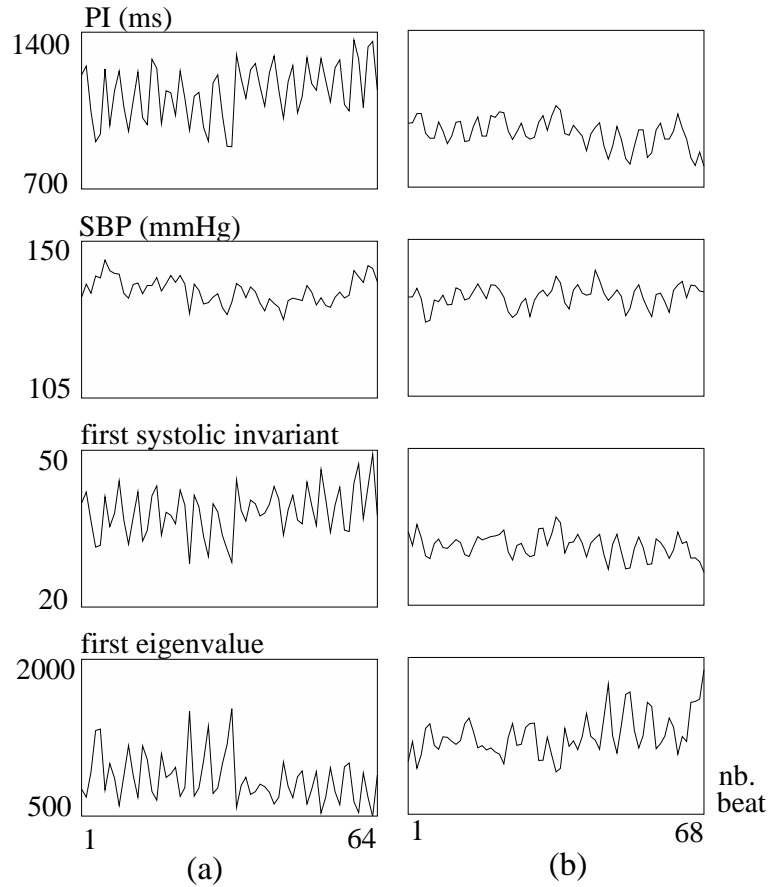


Figure 7: Time series of ABP parameters in a healthy subject under $0.25Hz$ paced breathing, in supine (a) and standing (b) positions after a 60 degrees tilt test. PI and $INVS_1$ are reduced whereas $|\lambda_1|$ is increased in the standing position, more than two minutes after the tilt test. SBP has the same level in both positions.

hypertension. Indeed, the ANS acts in the same way as in a dynamic exercise usually characterized by an increase in muscle oxygen needs. The isometric exercise is a form of exercise involving the static contraction of a muscle without any visible movement in the angle of the joints [13].

A group of 13 healthy subjects was considered. The continuous ABP was measured at the finger with a Finapres device [45]. The two conditions: at rest and during the handgrip

Table 1: ABP parameters during tilt protocol in 15 healthy subjects

| ABP parameters | supine | standing | probability |
|-------------------|------------|------------|-------------|
| Direct | | | |
| PI | 918 ± 33 | 778 ± 21 | *** |
| SBP | 121 ± 4 | 127 ± 3 | NS |
| DBP | 68 ± 4 | 80 ± 3 | ** |
| Eigenvalues | | | |
| First | 1515 ± 131 | 1965 ± 137 | *** |
| Second | 1205 ± 86 | 1612 ± 92 | *** |
| First invariants | | | |
| Global | 77 ± 6 | 71 ± 4 | NS |
| Systolic | 21 ± 1 | 19 ± 1 | ** |
| Diastolic | 56 ± 4 | 51 ± 3 | NS |
| Second invariants | | | |
| Global | 7041 ± 975 | 6833 ± 711 | NS |
| Systolic | 2705 ± 328 | 2566 ± 247 | NS |
| Diastolic | 4336 ± 648 | 4276 ± 465 | NS |

Data are expressed as means and SEM; **: $P \leq .01$; ***: $P \leq .001$

Table 2: Beat-to-beat BRS during tilt protocol

| | supine | tilt | standing | probability |
|-------|-------------|-------------|--------------|-------------|
| R^2 | .335 ± .102 | .611 ± .074 | .421 ± .079 | *** |
| slope | -.105 ± .03 | -.177 ± .03 | -.106 ± .015 | ** |

R^2 and slope of the linear regression between $|\lambda_1(n)|$ and $PI(n+1)$, over about 60 beats, in 9 healthy subjects. Data are expressed as means and SEM; ** $p \leq .01$; *** $p \leq .001$, at repeated measures analysis of variance. Slope and R^2 are the strongest during tilt.

Table 3: Three indices of beat-to-beat BRS during tilt

| R^2 | tilt |
|---------------|-------------|
| $ \lambda_1 $ | .611 ± .074 |
| SBP | .351 ± .091 |
| PP | .415 ± .069 |

Mean of R^2 of the linear regression between ABP parameters ($|\lambda_1|$, SBP, PP) and PI , over about 60 beats, in 9 healthy subjects of the tilt test. Data are expressed as means and SEM. $|\lambda_1|$ is the most strongly correlated with PI .

test, were compared using the Wilcoxon non parametric paired test.

In Fig. 9, the time series of PI , SBP , $INVS_2$ and $|\lambda_1|$ are presented at rest and during the handgrip test. Table 4 illustrates the mean levels of the ABP parameters. We notice that while all the first invariants do not change significantly, the second invariants are sensitively

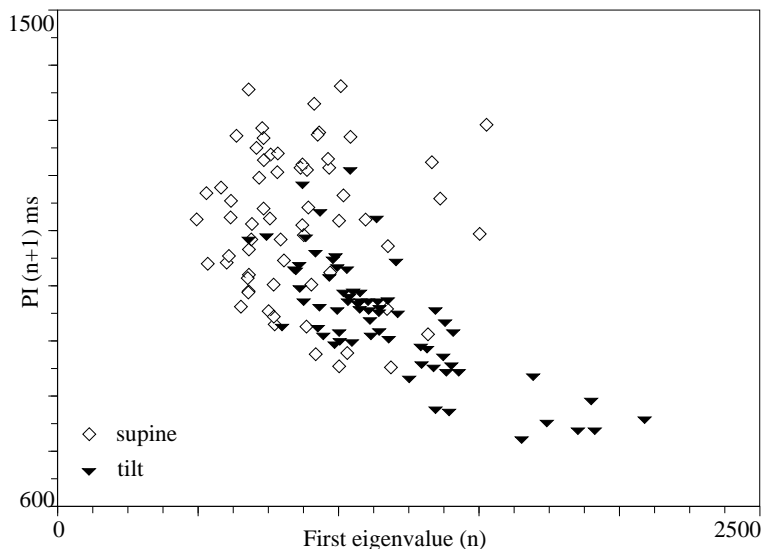


Figure 8: Beat-to-beat BRS, represented as the relation between $|\lambda_1(n)|$ and $PI(n+1)$. Slope and correlation are stronger during tilt.

increased during handgrip.

The voluntary central command, involved in the handgrip, synchronously activates the motor and CV systems, leading first to an increase in the heart rate, followed by an increase in the ABP [22], [30]. So, as expected, PI decreases and SBP increases (Table 4). Moreover, $INVS_1$ might inform us that SV does not change while $INVS_2$ might inform us about the increasing contractility, as if the heart tries to eject the same quantity of blood during a smaller period. Such a result evokes the *treppe effect* (or frequency-force relation), where an increase in heart rate indirectly induces an increase in contractility.

As in the case of the tilt test, we study the relationship between PI and $|\lambda_1|$. Fig. 10 illustrates the relation between PI of the beat $n+1$ and $|\lambda_1|$ computed for the beat n at rest and during the handgrip test. The strong linear correlation between PI and $|\lambda_1|$ is the same at rest and during the handgrip, but the slope is significantly lower during the handgrip (Table 5). Moreover, a comparison with usual BRS indices, SBP and PP, shows that $|\lambda_1|$ has the strongest correlation with PI (Table 6). This result, as obvious as in the case of the tilt test leads us to consider $|\lambda_1|$ as a promising index that can be used to study the relation between the heart period and ABP.

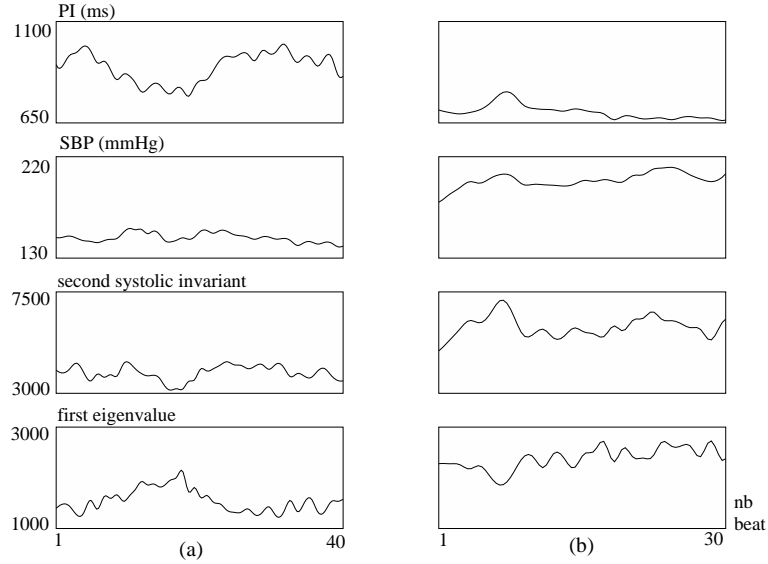


Figure 9: Time series of ABP parameters in a healthy subject under spontaneous breathing, at rest (a) and during the handgrip test (b). PI is reduced whereas SBP, $INV S_2$ and $|\lambda_1|$ are strongly increased during handgrip.

Table 4: ABP parameters during handgrip protocol in 13 healthy subjects

| ABP parameters | rest | handgrip | probability |
|-------------------|-------------|--------------|-------------|
| Direct | | | |
| PI | 953 ± 59 | 748 ± 42 | *** |
| SBP | 148 ± 5 | 183 ± 5 | *** |
| DBP | 83 ± 3 | 104 ± 4 | *** |
| Eigenvalues | | | |
| First | 1439 ± 160 | 2325 ± 249 | ** |
| Second | 1186 ± 125 | 1872 ± 180 | *** |
| First invariants | | | |
| Global | 96 ± 6 | 95 ± 6 | NS |
| Systolic | 26 ± 1 | 26 ± 1 | NS |
| Diastolic | 70 ± 4 | 69 ± 4 | NS |
| Second invariants | | | |
| Global | 10239 ± 866 | 12886 ± 1192 | ** |
| Systolic | 3956 ± 344 | 5013 ± 470 | ** |
| Diastolic | 6283 ± 526 | 7872 ± 727 | ** |

Data are expressed as means and SEM; ** $p \leq .01$; *** $p \leq .001$.

Table 5: Beat-to-beat BRS during handgrip protocol

| | rest | handgrip | probability |
|-------|--------------|--------------|-------------|
| R^2 | .647 ± .054 | .609 ± .050 | NS |
| slope | -.302 ± .071 | -.132 ± .024 | ** |

R^2 and slope of the linear regression between $|\lambda_1(n)|$ and $PI(n + 1)$, over about 40 beats, in 13 healthy subjects. Data are expressed as means and SEM; ** $p < .01$; *** $p < .001$, at paired test. Slope is reduced during handgrip whereas R^2 is not significantly different.

Table 6: Three indices of beat-to-beat BRS during handgrip protocol

| R^2 | rest | handgrip |
|---------------|-------------|-------------|
| $ \lambda_1 $ | .647 ± .054 | .609 ± .050 |
| SBP | .166 ± .055 | .261 ± .060 |
| PP | .375 ± .078 | .284 ± .060 |

Mean R^2 of the linear regression between ABP parameters ($|\lambda_1|$, SBP, PP) and PI , over about 40 beats, in the 13 healthy subjects of the handgrip test. Data are expressed as means and SEM. $|\lambda_1|$ is the most strongly correlated with PI .

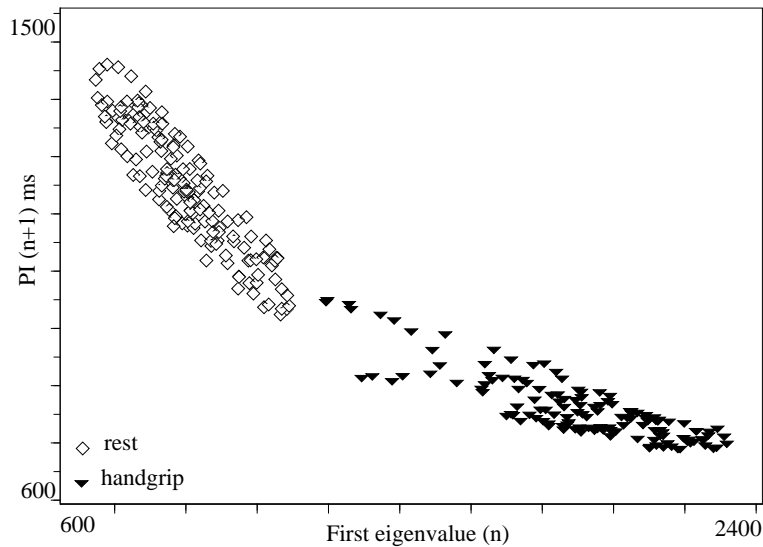


Figure 10: Beat-to-beat BRS, represented as the relation between $|\lambda_1(n)|$ and $PI(n + 1)$. Slope is lower during handgrip.

5 Conclusion

This article deals with a new ABP analysis method based on the scattering theory. This SBSA method can be thought of as a nonlinear Fourier analysis for pulse-like signals. It allows analysis and precise reconstruction as is shown by the very good agreement between real and estimated pressures. We have also presented an application to a filtering problem consisting in separating the systolic and diastolic phases. Then, we have introduced new cardiovascular indices computed with the SBSA method. These parameters include the first two systolic invariants and we think that they might give information on the variation of the stroke volume and the ventricular contractility, that are difficult to measure routinely. Another interesting parameter is the first eigenvalue which seems to reflect the BRS in a certain way. The results obtained from the analysis of two widely used physiological conditions are promising and we are now working on the validation of the advanced hypotheses.

References

- [1] T. Aktosun and M. Klaus. Chapter 2.2.4, inverse theory: problem on the line. In *E.R. Pike and P.C. Sabatier, Scattering*, pages 770–785. Academic Press, London, 2001.
- [2] M. Baumert, L. Brechtel, J. Lock, M. Hermsdorf, R. Wolff, V. Baier, and A. Voss. Heart rate variability, blood pressure variability, and baroreflex sensitivity in overtrained athletes. *Clin. J. Sport. Med.*, 15(5):412–417, September 2006.
- [3] J. Bestel, L. Mangin, C. Médigue, A. Monti, and M. Sorine. Proposition of an index of the autonomic nervous system activity in the arterial blood pressure short term regulation. *Blood Pressure Variability in Health and Disease, Satellite Symposium of the XVII^e Scientific Meeting of the International Society of Hypertension*, 12/Suppl. 1 of the Fundamental & Clinical Pharmacology journal, Nancy, June 1998.
- [4] Ph. Blanchard and J. Stubbe. Bound states for Schrödinger hamiltonians: phase space methods and applications. *Rev. Math. Phys.*, 35:504–547, 1996.
- [5] E. J Bowers and A. Murray. Effects on baroreflex sensitivity measurements when different protocols are used to induce regular changes in beat-to-beat intervals and systolic pressure. *Physiol. Meas.*, 25:523–538, 2004.
- [6] F. Calogero and A. Degasperis. *Spectral Transform and Solitons*. North Holland, 1982.
- [7] K. Chadan and P. C. Sabatier. *Inverse problems in quantum scattering theory*. Springer, New York, 2nd edition, 1989.
- [8] A. Charloux, E. Lonsdorfer-Wolf, R. Richard, E. Lampert, M. Oswald-Mammosser, B. Mettauer, B. Geny, and J. Lonsdorfer. A new impedance cardiograph device for the non-invasive evaluation of cardiac output at rest and during exercise: comparison with the direct Fick method. *Eur. J. Appl. Physiol.*, 82(4):313–320, July 2000.
- [9] E. Crépeau and M. Sorine. A reduced model of pulsatile flow in an arterial compartment. *Chaos Solitons & Fractals*, 34:594–605, 2007.
- [10] T. L. Culham and G. K. Savard. Hemodynamic strategies in blood pressure regulation during orthostatic challenge in women. *Revue canadienne de physiologie appliquée*, 22(4):351–367, 1997.
- [11] P. A. Deift and E. Trubowitz. Inverse scattering on the line. *Communications on Pure and Applied Mathematics*, XXXII:121–251, 1979.
- [12] W. Eckhaus and A. Vanhartem. *The Inverse Scattering Transformation and the Theory of Solitons*. North-Holland, 1983.
- [13] U. Freyschuss. Cardiovascular adjustment to somatomotor activation. The elicitation of increments in heart rate, aortic pressure and venomotor tone with the initiation of muscle contraction. *Acta Physiol Scand Suppl*, 342:01–63, 1970.

-
- [14] C. S. Gardner, J. M. Greene, M. D. Kruskal, and R. M. Miura. Korteweg-de Vries equation and generalizations VI. Methods for exact solution. In *Communications on pure and applied mathematics*, volume XXVII, pages 97–133. J.Wiley & sons, 1974.
- [15] I. M. Gel’fand and B. M. Levitan. On the determination of a differential equation from its spectral function. *Amer. Math. Soc. Transl.*, 2(1):253–304, 1955.
- [16] F. Gesztesy and H. Holden. Trace formulas and conservation laws for nonlinear evolution equations. *Reviews in Mathematical Physics*, 6(1):51–95, 1994.
- [17] J. Gorcsan, D. P. Strum, W. A. Mandarino, V. K. Gulati, and M. R. Pinsky. Quantitative assessment of alterations in regional left ventricular contractility with color-coded tissue doppler echocardiography. Comparison with sonomicrometry and pressure-volume relations. *Circulation*, 95:2423–2433, 1997.
- [18] N. L. Greenberg, M. S. Firstenberg, P. L. Castro, M. Main, A. Travaglini, J. A. Odabashian, J. K. Drinko, L. L. Rodriguez, J. D. Thomas, and M. J. Garcia. Doppler-derived myocardial systolic strain rate is a strong index of left ventricular contractility. *Circulation*, 105:99–105, 2002.
- [19] M. P. M. Harms, K. H. Wesseling, F. Pott, M. Jenstrup, J. Van Goudoever, N. H. Secher, and J. J. Van Lieshout. Continuous stroke volume monitoring by modelling flow from non-invasive measurement of arterial pressure in humans under orthostatic stress. *Clinical Science*, 97:291–301, 1999.
- [20] B. Helffer and D. Robert. Riesz means of bound states and semiclassical limit connected with a Lieb-Thirring conjecture II. *Ann. de l’Inst. H. Poincaré*, 53(2):139–147, 1990.
- [21] B. Helffer and D. Robert. Riesz means of bound states and semiclassical limit connected with a Lieb-Thirring’s conjecture I. *Asymptotic Analysis*, 3:91–103, 1990.
- [22] S. F. Hobbs. Central command during exercise: parallel activation of the cardiovascular and motor systems by descending command signals. In *Circulation, Neurobiology, and Behavior*, pages 2176–232. 1982.
- [23] D. Kozłowski, P. Byrdziak, W. Krupa, M. Gawrysiak, G. Piwko, J. Kubica, and G. Swiatecka. Left ventricle systolic volume in vasovagal syncope patients. *Folia Morphol (Warsz)*, 62(3):175–178, 2003.
- [24] T. M. Laleg, E. Crépeau, and M. Sorine. Separation of arterial pressure into a nonlinear superposition of solitary waves and a windkessel flow. *To appear in Biomedical Signal Processing and Control Journal*. Available online at <http://dx.doi.org/10.1016/j.bspc.2007.05.004>.
- [25] T. M. Laleg, E. Crépeau, and M. Sorine. Travelling-wave analysis and identification. A scattering theory framework. In *Proc. European Control Conference ECC, Kos, Greece*, July 2007.

- [26] A. Laptev and T. Weidl. Sharp Lieb-Thirring inequalities in high dimensions. *Acta Mathematica*, 184(1):87–111, 2000.
- [27] R. D. Lipman, J.K. Salisbury, and J. A. Taylor. Spontaneous indices are inconsistent with arterial baroreflex gain. *Hypertension*, 42(4):481–487, 2003.
- [28] L. Mangin, A. Monti, C. Médigue, I. Macquin-Mavier, M. E. Lopes, P. Gueret, A. Castaigne, B. Swynghedauw, and P. Mansier. Altered baroreflex gain during voluntary breathing in chronic heart failure. *European Journal of Heart Failure*, 3:189–195, 2001.
- [29] V. A. Marchenko. *Strum-Liouville operators and applications*. Birkhäuser, Basel, 1986.
- [30] D. I. McCloskey. Centrally-generated commands and cardiovascular control in man. *Clin. Exp. Hypertens.*, 3(3):369–378, 1981.
- [31] P. D. Miller and S. R. Clarke. An exactly solvable model for the interaction of linear waves with Korteweg-de Vries solitons. *SIAM J. MATH. ANAL.*, 33(2):261–285, 2001.
- [32] S. Molchanov, M. Novitskii, and B. Vainberg. First KdV integrals and absolutely continuous spectrum for 1-d Schrödinger operator. *Commun. Math. Phys*, 216:195–213, 2001.
- [33] A. Monti, C. Médigue, and L. Mangin. Instantaneous parameter estimation in cardiovascular time series by harmonic and time-frequency analysis. *IEEE Transactions on Biomedical Engineering*, 49(12):1547–1556, December 2002.
- [34] A. Monti, C. Médigue, H. Nedelcoux, and P. Escourrou. Cardiovascular autonomic control during sleep in normal subjects. *European Journal of Applied Physiology*, 87(2):174–181, 2002.
- [35] J. F. Paquerot and M. Remoissenet. Dynamics of nonlinear blood pressure waves in large arteries. *Physics Letters A*, pages 77–82, October 1994.
- [36] J. Parlow, J. P. Viale, G. Annat, R. Hughson, and L. Quintin. Spontaneous cardiac baroreflex in humans. Comparison with drug-induced responses. *Hypertension*, 25(5):1058–1068, May 1995.
- [37] R. J. Parmer, J. H. Cervenka, and R. A. Stone. Baroreflex sensitivity and heredity in essential hypertension. *Circulation*, 85:497–503, 1992.
- [38] M. Remoissenet. *Waves called solitons, concepts and experiments*. Springer, 3rd edition, 1999.
- [39] A. C. Scott, F. Y. F. Chu, and D. W. McLaughlin. The soliton: A new concept in applied science. *Proceedings of the IEEE*, 61(10):1443–1483, October 1973.
- [40] P. Segers and P. Verdonck. *Principles of Vascular Physiology*, chapter 6, pages 116–137. Panvascular Medecine. Integrated Clinical Managements. Springer Verlag, 2002.

-
- [41] J. K. Shoemaker, C. S. Hogeman¹, and L. I. Sinoway. Contributions of msna and stroke volume to orthostatic intolerance following bed rest. *Am. J. Physiol. Regul. Integr. Comp. Physiol.*, 277:R1084–R1090, 1999.
- [42] J. Siebert, P. Drabik, R. Lango, and K. Szyndler. Stroke volume variability and heart rate power spectrum in relation to posture changes in healthy subjects. *Medical Science Monitor*, 10(2):MT31–MT37, 2004.
- [43] B. Takase, H. Hosaka, K. Kitamura, A. Uehata, K. Satomura, K. Isojima, S. Kosuda, S. Kusano, A. Kurita, and F. Ohsuzu. The repeatability of left ventricular volume assessment by a new ambulatory radionuclide monitoring system during head-up tilt. *Jpn. Heart J.*, 42(6):749–758, November 2001.
- [44] I. Taneja, C. Moran, M. S. Medow, J. L. Glover, L. D. Montgomery, and J. M. Stewart. Differential effects of lower body negative pressure and upright tilt on splanchnic blood volume. *m. J. Physiol. Heart. Circ. Physiol.*, 292:H1420–H1426, 2007.
- [45] K. H. Wesseling. Method and device for controlling the cuff pressure in measuring the blood pressure in a finger by means of photo-electric plethysmograph. *United State Patent*, September 1985.
- [46] N. Westerhof, P. Sipkema, G. C. Van Den Bos, and G. Elzinga. Forward and backward waves in the arterial system. *Cardiovascular Research*, 6:648–656, 1972.
- [47] M. F. Wilson, B. H. Sung, G. A. Pincomb, and W. R. Lovallo. Simultaneous measurement of stroke volume by impedance cardiography and nuclear ventriculography: comparisons at rest and exercise. *Ann. Biomed. Eng.*, 17(5):475–482, 1989.
- [48] S. Yomosa. Solitary waves in large vessels. *Journal of the Physical Society of Japan*, 50(2):506–520, February 1987.
- [49] N. J. Zabusky and M. D. Kruskal. Interaction of 'soliton' in a collisionless plasma and the recurrence of initial states. *Physical Review Letters*, 15(6):240–243, 1965.



Unité de recherche INRIA Rocquencourt
Domaine de Voluceau - Rocquencourt - BP 105 - 78153 Le Chesnay Cedex (France)

Unité de recherche INRIA Futurs : Parc Club Orsay Université - ZAC des Vignes
4, rue Jacques Monod - 91893 ORSAY Cedex (France)

Unité de recherche INRIA Lorraine : LORIA, Technopôle de Nancy-Brabois - Campus scientifique
615, rue du Jardin Botanique - BP 101 - 54602 Villers-lès-Nancy Cedex (France)

Unité de recherche INRIA Rennes : IRISA, Campus universitaire de Beaulieu - 35042 Rennes Cedex (France)

Unité de recherche INRIA Rhône-Alpes : 655, avenue de l'Europe - 38334 Montbonnot Saint-Ismier (France)

Unité de recherche INRIA Sophia Antipolis : 2004, route des Lucioles - BP 93 - 06902 Sophia Antipolis Cedex (France)

Éditeur
INRIA - Domaine de Voluceau - Rocquencourt, BP 105 - 78153 Le Chesnay Cedex (France)
<http://www.inria.fr>
ISSN 0249-6399